Ceramics International 47 (2021) 28487–28492

Contents lists available at ScienceDirect

Ceramics International

journal homepage: www.elsevier.com/locate/ceramint

The effect of co-substitution on the microwave dielectric properties of $Ba_{6-3x}Nd_{8+2x}Ti_{18}O_{54}$($x$=2/3) ceramics

Jin Huang [a,1], Geng Wang [a,c,1], Mei Wang [a], Syed ul Hasnain Bakhtiar [a], Longhui Zha [a], Ming Hu [a], Nan Nie [a], Qiuyun Fu [a,b,*]

[a] School of Optical and Electronic Information, Engineering Research Center for Functional Ceramics of the Ministry of Education, Huazhong University of Science and Technology, Wuhan 430074, PR China
[b] Shenzhen Huazhong University of Science and Technology Research Institute, Shenzhen 518000, PR China
[c] School of Electronic Information and Engineering, Hubei University of Science and Technology, Xianning 437100, PR China

ARTICLE INFO

Keywords:
Microwave dielectric ceramics
Tungsten bronze
A/B-site co-substitution

ABSTRACT

In this work, the microwave dielectric properties of $Ba_4(Nd_{1-y}Bi_y)_{28/3}Ti_{18-x}(Al_{1/2}Ta_{1/2})_xO_{54}$($0\leq x\leq 2$, $0.05\leq y\leq 0.2$) ceramics co-substituted by A/B-site were studied. Firstly, $(Al_{1/2}Ta_{1/2})^{4+}$ was used for substitution at B-site. At $0\leq x\leq 1.5$, the above mentioned ceramic was found to exist in single-phase tungsten bronze structure, but at $x = 2.0$, the secondary phase appeared. Although the dielectric constant decreased by doping the $(Al_{1/2}Ta_{1/2})^{4+}$, but the quality factor was observed to improve by 40% and the temperature coefficient of resonant frequency decreased by 75%. Based on the above results, Bi^{3+} was introduced to $Ba_4Nd_{28/3}Ti_{17}(Al_{1/2}Ta_{1/2})O_{54}$. The introduction of Bi^{3+} reduced the sintering temperature, greatly improved the dielectric constant, and ultimately decreased the temperature coefficient of resonant frequency, but it led to deterioration of quality factor. At last, with appropriate site-substitution content control ($x = 1.0$,$y = 0.15$), excellent comprehensive properties ($\varepsilon_r = 89.0$, $Q \times f = 5844$ GHz @ 5.89 GHz , TCF = +8.7 ppm/°C) were obtained for the samples sintered at 1325 °C for 4 h.

1. Introduction

Microwave dielectric ceramics are the key materials in microwave band communication [1,2]. With the rapid development of communication technology, the microwave dielectric material must own following essential parameters: (1) high ε_r; (2) high $Q \times f$ value; (3) near-zero TCF value [3,4]. $Ba_{6-3x}Nd_{8+2x}Ti_{18}O_{54}$ (BNT)ceramics exhibit enhanced microwave dielectric properties ($\varepsilon_r > 80$, $Q \times f > 5000$ GHz, TCF = +50-+150 ppm/°C), most suitable for mobile communication equipment [5,6], and is widely been concerned by researchers. But the relatively high resonant frequency temperature coefficient seriously limits its application in communication devices. BNT ceramic exhibits a tungsten bronze structure [7], connected by the common vertex of oxygen octahedron to form an unfilled space network. And it has been proved that the quality factor is the highest at $x = 2/3$ in $Ba_{6-3x}Nd_{8+2x}Ti_{18}O_{54}$ ceramics [8]. Huge research has been done on tuning the properties of BNT ceramics by modification of framework through substitution. For example, employing Ca^{2+} or Sr^{2+} atoms to replace Ba^{2+} in the A2 site of BNT ceramics can improve the dielectric constant of the ceramic system, but unfortunately at the instance, the temperature coefficient of resonant frequency will increase [9]. In another study, Nd^{3+} at A1 site is replaced by Bi^{3+} and Sm^{3+}, it is assumed that this kind of substitution can effectively decrease the temperature coefficient of resonant frequency [10–14]. Furthermore, for Bi^{3+} substitution, it can also improve the dielectric constant of the ceramic materials. While in the case of B-site substitution, Al^{3+}, Sn^4, Zr^{4+}, $(Al_{1/2}Nb_{1/2})^{4+}$ and $(Cr_{1/2}Nb_{1/2})^{4+}$ substitution were observed in literature [15–19], which proven that B-site substitution can effectively adjust the quality factor and resonant frequency temperature coefficient of ceramic materials. Theoretically, the A/B-site co-substitution can regulate the comprehensive microwave dielectric properties of ceramics in much better way.

Considering that by employing the $(Al_{1/2}Nb_{1/2})^{4+}$ for B site substitution has achieved good experimental results [19], as the Ta^{5+} and

* Corresponding author. School of Optical and Electronic Information, Engineering Research Center for Functional Ceramics of the Ministry of Education, Huazhong University of Science and Technology, Wuhan 430074, PR China.
E-mail address: fuqy@mail.hust.edu.cn (Q. Fu).
[1] these authors contribute equally as the first author.

https://doi.org/10.1016/j.ceramint.2021.07.003
Received 9 May 2021; Received in revised form 19 June 2021; Accepted 1 July 2021
Available online 2 July 2021

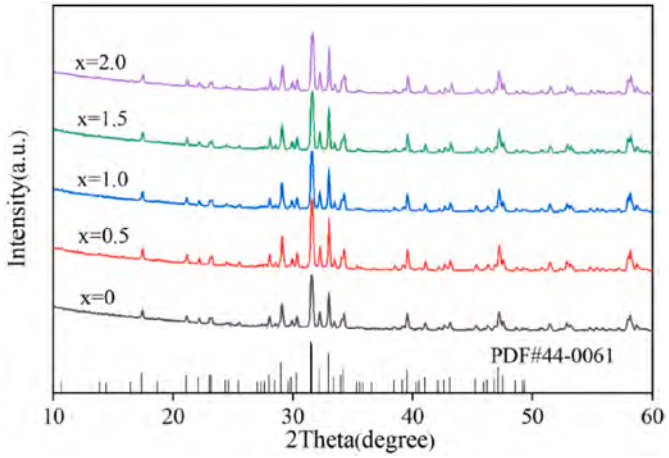

Fig. 1. X-ray diffraction pattern of $Ba_4Nd_{28/3}Ti_{18-x}(Al_{1/2}Ta_{1/2})_xO_{54}(0\leq x\leq 2)$ ceramics with different value of x.

Nb^{5+} exhibits similar ion radius, and Bi^{3+} can significantly regulate the microwave dielectric properties. This article focus on the A/B-site $Bi^{3+}/(Al_{1/2}Ta_{1/2})^{4+}$ co-substitution in $Ba_4Nd_{28/3}Ti_{17}(Al_{1/2}Ta_{1/2})O_{54}$ ceramic. The chemical formula presenting the co-doped ceramic is represented as $Ba_4(Nd_{1-y}Bi_y)_{28/3}Ti_{18-x}(Al_{1/2}Ta_{1/2})_xO_{54}(0\leq x\leq 2, 0.05\leq y\leq 0.2)$.

2. Experimental procedure

The $Ba_4(Nd_{1-y}Bi_y)_{28/3}Ti_{18-x}(Al_{1/2}Ta_{1/2})_xO_{54}(0\leq x\leq 2,\ 0.05\leq y\leq 0.2)$ ceramic samples were prepared by traditional solid-state method. High purity $BaCO_3$ (99.8%), Nd_2O_3 (99.99%), Bi_2O_3 (99.9%), TiO_2 (99.84%), Al_2O_3 (99.99%) and Ta_2O_5 (99.99%) were used as raw materials. The above powders were ball-milled in nylon jars having zirconia balls for 2 h in deionized water as a solvent medium. After drying the sample, the powder is calcined for 4 h duration, where the B site substituted samples were calcined at 1150 °C and the A/B-site co-substituted samples were calcined at 1100 °C at the rate of 5 °C/min. After another trial of ball milling and drying, 6 wt% polyvinyl alcohol (PVA) was added to the fine powder, ground and sieved at 60 mesh size and finally pressed into the steel mould (8 mm in diameter and 2–6 mm in thickness). At last, the samples were dwelled at 600 °C for 2 h to remove the organic binder. The B site substituted samples were sintered at 1350°C–1450 °C for 4 h and the A/B-site co-substituted samples were sintered at 1275°C–1375 °C for 4 h, at the rate of 5 °C/min.

The crystal structure was measured by X-ray diffraction (XRD) spectrometer using Cu Kα1 radiation (X'pert pro MPD, PANanlytical B. V., Netherlands). The microstructure of ceramics was analyzed by scanning electron microscope (SEM, Gemini SEM 300, Carl Zeiss, Germany), and energy dispersive spectrometry (EDS, X-MAX, Oxford) at the same time. Raman spectra were recorded using a Raman spectrometer (Horiba HR800, France), excited by a Nd/YAG laser (523 nm). Dielectric properties of samples at microwave frequency were measured by taking the advantage of the $TE_{01\delta}$ dielectric resonator method with a network analyzer (E5071C, Agilent). The TCF value was calculated using Eq. (1):

$$TCF = \frac{(f_{85} - f_{25}) \times 10^6}{(85-25) f_{25}} (ppm/^\circ C) \quad (1)$$

In Eq. (1), the f_{25} and f_{85} represent the resonant frequency at 25 °C and 85 °C, respectively.

3. Results and discussions

3.1. $(Al_{1/2}Ta_{1/2})^{4+}$ substitution for Ti^{4+}

Fig. 1 shows the XRD patterns for $Ba_4Nd_{28/3}Ti_{18-x}(Al_{1/2}Ta_{1/2})_xO_{54}(0\leq x\leq 2)$ ceramics sintered at 1400 °C for 4 h. It can be seen that the XRD patterns for all the samples fully match the PDF card of $BaNd_2Ti_4O_{12}$ (JCPDS No. 44–0061) showing a single tungsten bronze like structure [20]. However, a secondary phase was observed in the SEM image for the sample $x = 2.0$.

The surface microstructure and EDS analysis spectra of $Ba_4Nd_{28/3}Ti_{18-x}(Al_{1/2}Ta_{1/2})_xO_{54}$ $(0\leq x\leq 2)$ ceramics are shown in Fig. 2. The SEM images reveals that the samples have clear grains and typical columnar like grains with tungsten bronze structure. When $0\leq x\leq 1.5$, with increasing the amount of $(Al_{1/2}Ta_{1/2})^{4+}$ substitution, the average grain size of the sample increases, and no obvious changes were found in SEM images (BSE mode), indicating single-phase structure. At $x = 2.0$, a secondary phase appears in the SEM images, and the grain size was observed to get smaller. The phase composition of the secondary phase was analyzed by EDS which suggested that this secondary phase consists of high content of Al and Ta, and we can conclude that the upper limit of $(Al_{1/2}Ta_{1/2})^{4+}$ solid solution in ceramics is about $x = 1.5$.

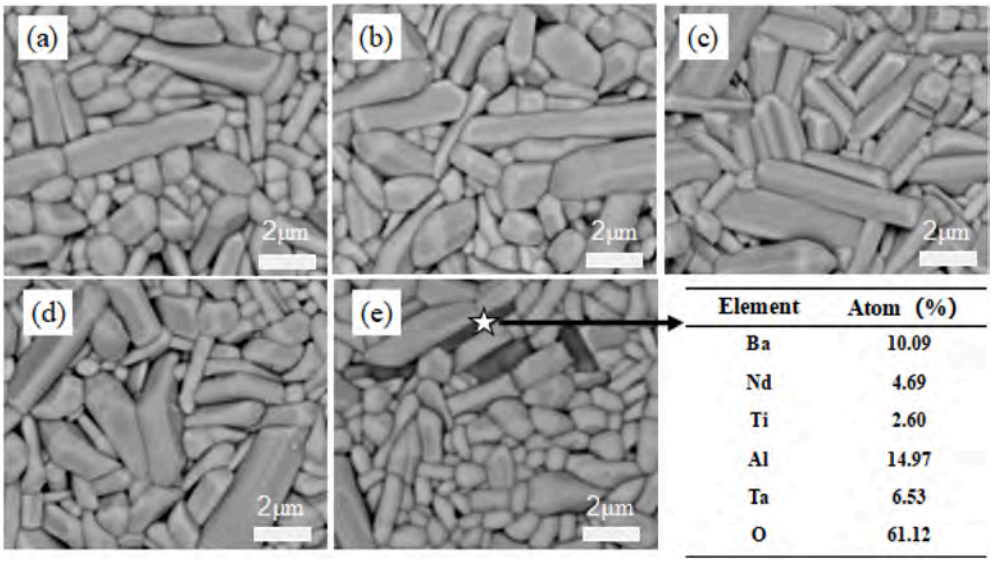

Fig. 2. SEM images of $Ba_4Nd_{28/3}Ti_{18-x}(Al_{1/2}Ta_{1/2})_xO_{54}(0\leq x\leq 2)$ ceramics sintered at 1400 °C for 4 h: where x is equal to (a) 0, (b) 0.5, (c) 1.0, (d) 1.5, (e) 2.0 and the table presents the EDS analysis of the secondary phase.

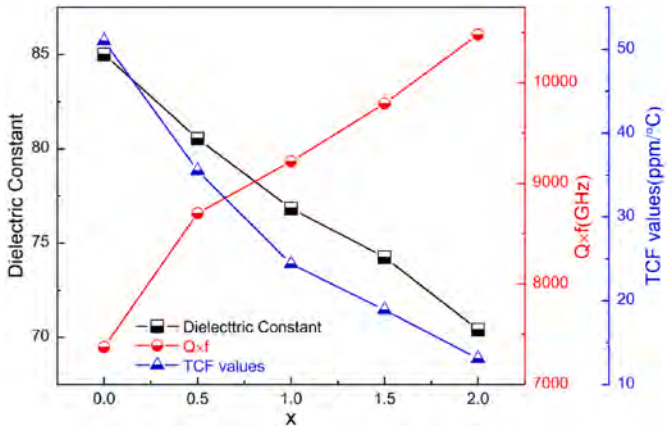

Fig. 3. Microwave dielectric properties of $Ba_4Nd_{28/3}Ti_{18-x}(Al_{1/2}Ta_{1/2})_xO_{54}(0\leq x\leq 2)$ ceramics with different $(Al_{1/2}Ta_{1/2})^{4+}$ substituting content.

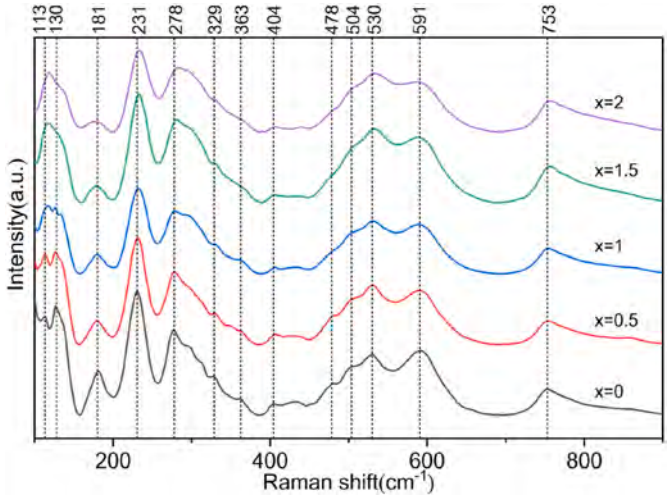

Fig. 4. Room-temperature Raman spectra of $Ba_4Nd_{28/3}Ti_{18-x}(Al_{1/2}Ta_{1/2})_xO_{54}(0\leq x\leq 2)$ ceramics.

Fig. 3 depicted the relationship between x value and microwave dielectric properties of $Ba_4Nd_{28/3}Ti_{18-x}(Al_{1/2}Ta_{1/2})_xO_{54}$ $(0\leq x\leq 2)$ ceramics. It was observed that, as the x value increased from 0 to 2.0, the dielectric constant of the ceramic dropped from 85.0 to 70.4, which is closely related to the ionic polarizability value. In this work, the low ionic polarizability of $(Al_{1/2}Ta_{1/2})^{4+}$(2.76 Å^3) compared with Ti^{4+}(2.93 Å^3) probably lead to decreasing an average ionic polarization and ultimately decreasing the dielectric constant [21,22]. The quality factor increased from 7400 GHz to 10,500 GHz, which is mainly related to the change in grain size as well as the secondary phase. At $0\leq x\leq 1.5$, the average size of the columnar like grains of the samples increased significantly, suggesting a corresponding decrease in grain-boundary densities. These grain boundaries will act as defects in the ceramic samples [23]. The decrease of grain-boundary densities will lead to ultimate decrease for dielectric loss of the ceramic sample, thus improving the quality factor. When $x = 2$, the proportion and size of grains decreased, and the secondary phase appears in sample, as can be seen in SEM images. The change in grain size and the appeared secondary phase combinedly affected the performance of the quality factor of the ceramics. The temperature coefficient at resonant frequency decreased from +51.2 ppm/°C to +13.1 ppm/°C, which is associated with the degree of oxygen octahedra tilting [24]. And the tilt degree of oxygen octahedron in $Ba_4Nd_{28/3}Ti_{18-x}(Al_{1/2}Ta_{1/2})_xO_{54}$ ceramics is analyzed by Raman spectra.

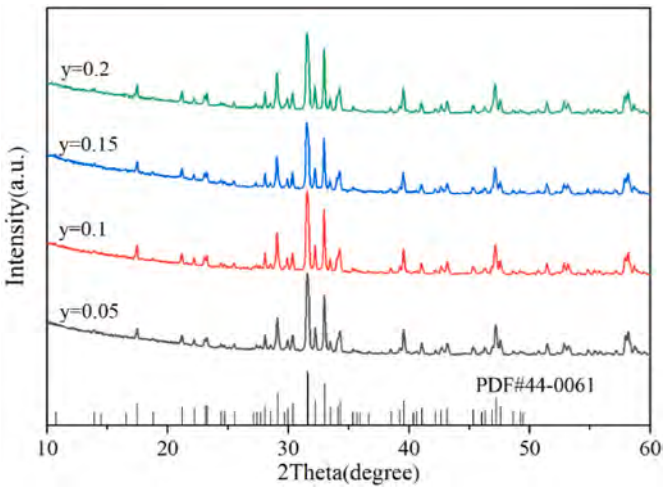

Fig. 5. X-ray diffraction of $Ba_4(Nd_{1-y}Bi_y)_{28/3}Ti_{17}(Al_{1/2}Ta_{1/2})O_{54}$ ceramics with different y value.

Raman spectroscopy is one of the powerful techniques for analysis of physical properties of oxygen octahedra and its arrangement [25]. Fig. 4 shows the Raman spectra over 100-900 cm^{-1} of $Ba_4Nd_{28/3}Ti_{18-x}(Al_{1/2}Ta_{1/2})_xO_{54}(0\leq x\leq 2)$ ceramics sintered at 1400 °C for 4 h. Total of 13 vibrational modes could be observed in the Raman spectra. The oxygen octahedra were tilting in $Ba_4Nd_{28/3}Ti_{18-x}(Al_{1/2}Ta_{1/2})_xO_{54}$ ceramics structure as compared with the perovskite structure, and the Raman spectra of $Ba_4Nd_{28/3}Ti_{18-x}(Al_{1/2}Ta_{1/2})_xO_{54}$ ceramics was found to be similar with the $CaTiO_3$ ceramics [26]. The Raman bands at 753 cm^{-1}, 591 cm^{-1}, 530 cm^{-1} and 504 cm^{-1} were attribute to be associated with the Ti–O symmetric stretching vibration, the 478 cm^{-1}, 404 cm^{-1} bands are related to the Ti–O bending vibration, while the Raman bands between 200 cm^{-1}-300 cm^{-1} were attributed to the rotation of the oxygen cage, and the bands in the 100 cm^{-1}-200 cm^{-1} region were connected to the translation movement of cation (Nd^{3+} and Ba^{2+}) in the A site [19,27].

As shown in Fig. 5, with increasing the x value, the Raman bands at 591 cm^{-1}, 530 cm^{-1}, 404 cm^{-1} was observed to get wider, which may be attributed to a reduction in the degree of B site order [28]. At the same time, the Raman bands at 231 cm^{-1}, 278 cm^{-1} become broadens, which indicates that the vibration associated with the rotation of the oxygen cage became weaker. This confirmed that flexible oxygen octahedra networks became stressed-rigid [29]. The intensity and width of Raman bands between 100 and 200 cm^{-1} changes obviously. This perhaps due to the vibration caused by A-site ions was restricted in stressed-rigid oxygen octahedra networks, and the lattice distortion caused by decrease of the unit cell volume. At the same time, the B sites is randomly occupied by Al^{3+} , Ti^{4+} and Ta^{5+}. Due to the difference in the ionic radius and force constant between B-site ions (Ti^{3+}, Al^{3+}, Ta^{5+}), the two adjacent oxygen octahedrons may be nonequivalent, which will lead to the corresponding increase in distortion and tilt degree of oxygen octahedron while absolute TCF value decreased [19]. The blue shift of the Raman bands at 753 cm^{-1}, 530 cm^{-1}, 278 cm^{-1}, 231 cm^{-1} indicates that the cell volume decreased when the substitution of $(Al_{1/2}Ta_{1/2})^{4+}$ increased.

3.2. Bi^{3+} substitution for Nd^{3+}

Based on above results, when $x = 1.0$, the ceramic shows an excellent comprehensive microwave dielectric properties: $\varepsilon_r = 76.8$, $Q\times f = 9217$ GHz(@ 6.17 GHz) , TCF = +24.4 ppm/°C, which is worthy of further study. Fig. 5 shows the XRD patterns of $Ba_4(Nd_{1-y}Bi_y)_{28/3}Ti_{17}(Al_{1/2}Ta_{1/2})O_{54}$ $(0.05\leq y\leq 0.2)$ ceramics. The diffraction peaks of ceramics with different amount of Bi^{3+} substitution matches the standard card (JCPDS

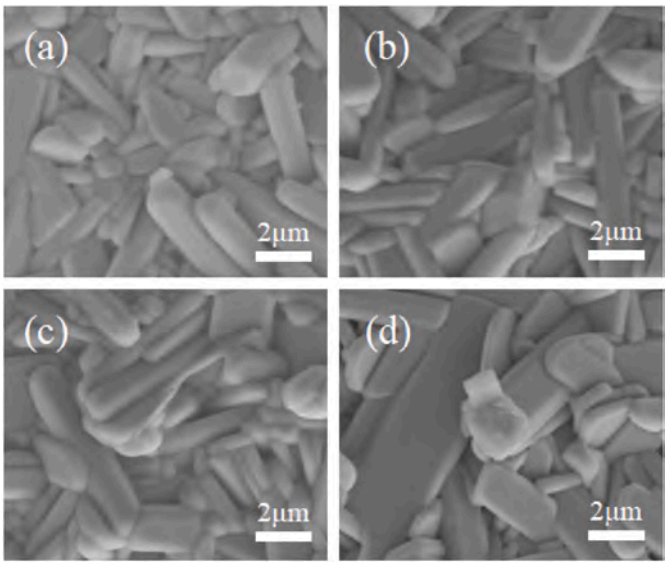

Fig. 6. SEM images of $Ba_4(Nd_{1-y}Bi_y)_{28/3}Ti_{17}(Al_{1/2}Ta_{1/2})O_{54}$ ($0.05 \leq y \leq 0.2$) ceramics: with y = (a) 0.05, (b) 0.1,(c) 0.15 and (d) 0.2.

No.44-0061), attributing to the single tungsten bronze structure [20].

From the SEM image shown in Fig. 6, it can be seen that the ceramic is composed of columnar like grains with tungsten bronze structure. However, with changing the amount of Bi^{3+} substitution, the surface morphology of the ceramic sample changed obviously. With increasing the y value, the abnormal growth of huge grains and the increase in liquid phase appeared in the samples. The reason is, the Bi_2O_3 melts (~800 °C) and converts to liquid phase at sintering temperature (1275 °C - 1375 °C), which can promote the ionic diffusion and further results in the acceleration of grain growth and the ultimate abnormal increase of the grain size. Fig. 7 shows the EDS surface scanning of the polished samples with $y = 0.05$ and 0.2. At $y = 0.05$, a uniform distribution of elements was observed at ceramic surface, without any aggregation; However, when $y = 0.2$, a secondary phase appeared in the ceramic sample. By scanning the surface, one can see that there are more Ti and Ba elements while less amount of Nd and Bi elements present in the secondary phase. It can be inferred that when the replaced amount of Bi increases, the sintering at high temperature causes a large amount of Bi volatilization, which leads to the deviation of the elemental proportion from the design composition, and the extra elements forms the

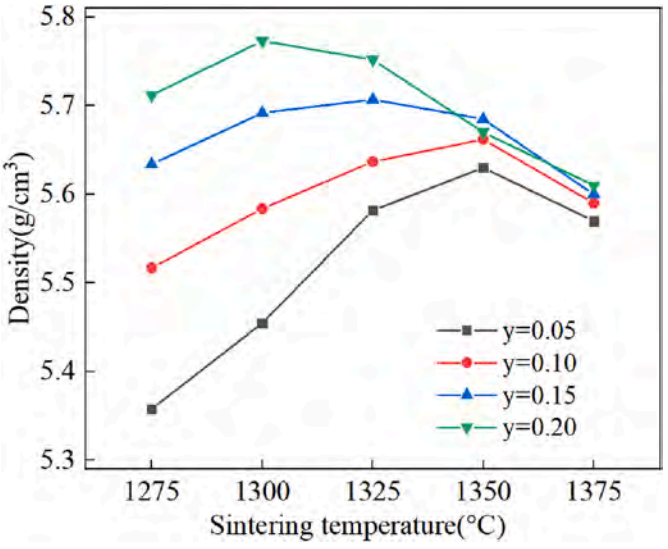

Fig. 8. Density of $Ba_4(Nd_{1-y}Bi_y)_{28/3}Ti_{17}(Al_{1/2}Ta_{1/2})O_{54}$ ($0.05 \leq y \leq 0.2$) ceramics sintered at different temperature.

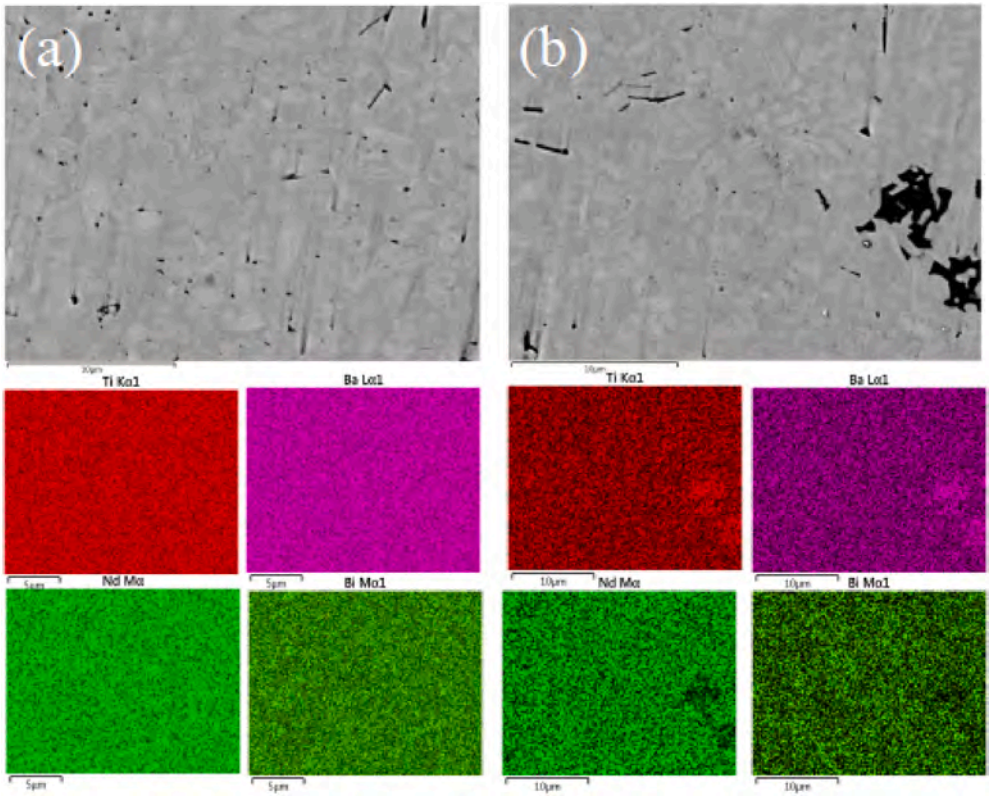

Fig. 7. EDS spectra of $Ba_4(Nd_{1-y}Bi_y)_{28/3}Ti_{17}(Al_{1/2}Ta_{1/2})O_{54}$ ($0.05 \leq y \leq 0.2$) ceramics: y = (a) 0.05, (b) 0.2.

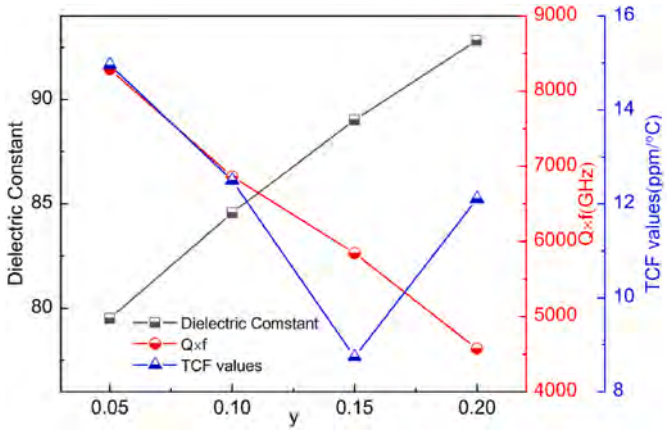

Fig. 9. Microwave dielectric properties of $Ba_4(Nd_{1-y}Bi_y)_{28/3}Ti_{17}(Al_{1/2}Ta_{1/2})O_{54}$ ($0.05 \le y \le 0.2$) ceramics with different Bi^{3+} substituting content.

secondary phase [13].

In Fig. 8, bulk densities versus y value of ceramics sintered at different temperatures were illustrated. Results shows an increase and an ultimate decrease in the density of all the samples. At the same time, it can be seen that with the increase of Bi^{3+} substitution, the optimal sintering temperature of the sample decreases from 1350 °C for y = 0.05 to 1300 °C for y = 0.2. The reason is, Bi_2O_3 exhibits low melting point, and forms a liquid phase during sintering process. The existence of the liquid phase is conducive to ion transfer and thus reduces the sintering temperature. With increasing the y value, the maximum density of the sample gradually increases, which may be due to the fact that atomic mass of Bi (208.98) is far greater than that of Nd (144.24). The liquid phase will fill up the pores during sintering, which improves the compactness and ultimate density of the ceramic sample [11].

Fig. 9 depicted the microwave dielectric properties of the samples. It was observed that, as the y increased from 0.05 to 0.2, the dielectric constant also increased continuously from 79.5 to 92.8. The ionic polarizability of Bi^{3+} was also observed to be greater than that of Nd^{3+}, which is 6.12 $Å^3$ and 5.01 $Å^3$, respectively and it will lead to the increase in ε_r value [21,22]. Furthermore, as the ionic radius of Bi^{3+} (~0.145 nm) is larger than that of Nd^{3+} (~0.127 nm), the moving space of Ti^{4+} located in the center of oxygen octahedron is enlarged, the coupling polarization between Ti^{4+} and surrounding O^{2-} is promoted, and also lead to the increase in dielectric constant [14]. With different trend, the introduction of Bi^{3+} seriously destroyed the quality factor of the sample, where the $Q \times f$ dropped from 8290 GHz to 4573 GHz. According to the above mentioned SEM images, with increasing y, the liquid phase of ceramic sample increases obviously, and the grains of the sample grow abnormally and the uniformity will also decreases, which will increase the probability of dislocation and other defects, thus increasing the dielectric loss and reducing the $Q \times f$ of the ceramic [14]. Furthermore, the TCF decreases from +15.0 ppm/°C to +8.7 ppm/°C, when y increases from 0.05 to 0.15, and TCF shows the value of +12.1 ppm/°C when the y reaches to 0.2. In the tungsten bronze ceramics, the temperature coefficient of resonant frequency (TCF) and the temperature coefficient of dielectric constant (τ_ε) changes in the opposite trend [30]. There is a lone pair of electrons on the outermost orbital (6 S) of Bi^{3+} ion, which has poor symmetry with the surrounding O^{2-}, and Bi^{3+} is easy to shift from the center to one end in the A site. With the increase of Bi^{3+} substitution, the lattice expands, the Bi^{3+} activity space becomes larger, and the polarization ability increases [31,32]. This "positive" dielectric constant temperature coefficient also indicates that the ceramic system has a "negative" resonant frequency temperature coefficient. When $y >$ 0.15, TCF begins to shift towards the positive direction, which may be related to the secondary phase and the greater liquid phase observed by SEM.

4. Conclusion

Appropriate content of bismuth and aluminum substitution in $Ba_4(Nd_{1-y}Bi_y)_{28/3}Ti_{18-x}(Al_{1/2}Ta_{1/2})_xO_{54}$ ($0 \le x \le 2, 0.05 \le y \le 0.2$) ceramics could improve the comprehensive performance. The introduction of $(Al_{1/2}Ta_{1/2})^{4+}$ improved the quality factor and reduced the temperature coefficient of the resonant frequency, but it resulted in the decrease in the dielectric constant. Its shortcomings were compensated by the introduction of Bi^{3+}, the temperature coefficient of resonance frequency was improved and the dielectric constant was also increased. At $x = 1.0$ and $y = 0.15$, the excellent microwave dielectric properties of ε_r = 89.0 , $Q \times f$ = 5844 GHz(@ 5.89 GHz) , TCF = +8.7 ppm/°C could be obtained.

Declaration of competing interest

The authors declare that they have no known competing financial interests or personal relationships that could have appeared to influence the work reported in this paper.

Acknowledgement

This work is supported by National Key Research and Development Plan (Grant No.2017YFB0406301) , Innovation Team Program of Hubei Province, China (Grant No.2019CFA004) , National Science Foundation of China (Grant No. 61971459) , Fund from Science, Technology and Innovation Commission of Shenzhen Municipality (Grant No. JCYJ20190809095009521) , and the Ph.D. research startup foundation of Hubei University of Science and Technology (Grant No. BK202109).

References

[1] C. Pei, J. Tan, Y. Li, et al., Effect of Sb-site nonstoichiometry on the structure and microwave dielectric properties of $Li_3Mg_2Sb_{1-x}O_6$ ceramics[J], Journal of Advanced Ceramics 9 (5) (2020) 588–594.
[2] F. Huang, H. Su, Y. Li, et al., Low-temperature sintering and microwave dielectric properties of $CaMg_{1-x}Li_{2x}Si_2O_6$(x=0–0.3) ceramics[J], Journal of Advanced Ceramics 9 (4) (2020) 471–480.
[3] G. Wang, Q. Fu, P. Guo, et al., Crystal structure, spectra analysis and dielectric characteristics of $Ba_4M_{28/3}Ti_{18}O_{54}$(M= La, Pr, Nd, and Sm) microwave ceramics [J], Ceram. Int. 47 (2) (2021) 1750–1757.
[4] J. Li, C. Zhang, H. Liu, et al., Structure, morphology, and microwave dielectric properties of $SmAlO_3$ synthesized by stearic acid route[J], Journal of Advanced Ceramics 9 (5) (2020) 558–566.
[5] H. Chen, B. Tang, Z. Xiong, et al., Microwave dielectric properties of aluminum-substituted Ba6− 3xNd8+ 2xTi18O54 ceramics[J], Int. J. Appl. Ceram. Technol. 13 (3) (2016) 564–568.
[6] H. Chen, B. Tang, X. Guo, et al., Effects of B-site substitution on microwave dielectric properties of $Ba_{6-3x}Nd_{8+2x}[Ti_{1-z}(Ni_{1/3}Nb_{2/3})_z]_{18}O_{54}$ ceramics[J], Int. J. Appl. Ceram. Technol. 12 (2015) E170–E175.
[7] R.G. Matveeva, M.B. Varfolomeev, L.S. Ilyushchenko, Refinement of the composition and crystal structure of $Ba_{3.75}Pr_{9.5}Ti_{18}O_{54}$[J], Zh. Neorg. Khim. 29 (1) (1984) 31–34.
[8] H. Ohsato, M. Imaeda, Y. Takagi, et al., Microwave quality factor improved by ordering of Ba and rare-earthon the tungsten bronze-type $Ba_{6-3x}R_{8+2x}Ti_{18}O_{54}$ (R=La, Nd and Sm) solid solutions[C]//ISAF 1998. Proceedings of the Eleventh IEEE International Symposium on Applications of Ferroelectrics, IEEE, 1998, pp. 509–512. Cat. No. 98CH36245.
[9] R. Ubic, I.M. Reaney, W.E. Lee, et al., Effect of divalent dopants on properties of $Ba_{3.75}Nd_{9.5}Ti_{18}O_{54}$ microwave dielectric resonators[J], MRS Online Proceedings Library Archive, 1996, p. 453.
[10] J.W. Yong, M.C. Xiang, Bismuth/samarium cosubstituted $Ba_{6-3x}Nd_{8+2x}Ti_{18}O_{54}$ microwave dielectric ceramics[J], J. Am. Ceram. Soc. 83 (7) (2000) 1837–1839.
[11] M. Long, W. Zhuang, B. Tang, et al., Microwave dielectric properties of $Ba_{0.75}Sr_{0.25}(Nd_xBi_{1-x})_2Ti_4O_{12}$ solid solution[J], Ceramics 55 (4) (2011) 373–377.
[12] T. Okawa, M. Imaeda, H. Ohsato, Microwave dielectric properties of Bi-added $Ba_4Nd_{9+1/3}Ti_{18}O_{54}$[J], Jpn. J. Appl. Phys. 39 (9) (2000) 5645–5649.
[13] M. Valant, D. Suvorov, Incorporation of bismuth into $Ba_{6-x}R_{8+2/3x}Ti_{18}O_{54}$(R = Nd, Gd)[J], J. Mater. Sci. 36 (12) (2001) 2991–2997.
[14] T. Okawa, M. Imaeda, H. Ohsato, et al., Site occupancy of Bi ions and microwave dielectric properties in Bi-doped $Ba_{6-3x}R_{8+2x}Ti_{18}O_{54}$(R = rare earth, x = 2/3) solid solutions[J], Mater. Chem. Phys. 79 (2–3) (2003) 199–203.
[15] H. Chen, B. Tang, Z. Xiong, et al., Microwave dielectric properties of aluminum-substituted $Ba_{6-3x}Nd_{8+2x}Ti_{18}O_{54}$ ceramics[J], Int. J. Appl. Ceram. Technol. 13 (3) (2016) 564–568.

[16] B. Huang, Z. Wang, T. Chen, et al., Microstructure and microwave dielectric properties of $Ba_{4.2}Nd_{9.2}Ti_{18-x}Sn_xO_{54}$(x= 0, 0.25, 0.5, 1, 1.5, 2) ceramics[J], J. Mater. Sci. Mater. Electron. 26 (5) (2015).
[17] Y.J. Wu, X.M. Chen, Dielectric ceramics of $Ba_{6-3x}Nd_{8+2x}$(Zr, Ti)$_{18}O_{54}$[J], Ferroelectrics 233 (1) (1999) 271–277.
[18] X. Guo, B. Tang, J. Liu, et al., Microwave dielectric properties and microstructure of $Ba_{6-3x}Nd_{8+2x}Ti_{18-y}(Cr_{1/2}Nb_{1/2})_yO_{54}$ ceramics[J], J. Alloys Compd. 646 (2015) 512–516.
[19] Z. Xiong, B. Tang, Z. Fang, et al., Crystal structure, Raman spectroscopy and microwave dielectric properties of $Ba_{3.75}Nd_{9.5}Ti_{18-z}(Al_{1/2}Nb_{1/2})_{(z)}O_{54}$ ceramics [J], J. Alloys Compd. 723 (2017) 580–588.
[20] X.H. Zheng, B.L. Liang, D.P. Tang, et al., Crystal structure and microwave dielectric properties of $Ba_4Nd_{9.33}Ti_{18}O_{54}$ ceramics with $Ca_{0.61}Nd_{0.26}TiO_3$ addition[J], J. Ceram. Soc. Jpn. 117 (1371) (2009) 1254–1257.
[21] R.D. Shannon, Dielectric polarizabilities of ions in oxides and fluorides[J], J. Appl. Phys. 73 (1) (1993) 348–366.
[22] G. Wang, Q. Fu, H. Shi, et al., Novel thermally stable, high quality factor $Ba_4(Pr_{0.4}Sm_{0.6})_{28/3}Ti_{18-y}Ga_{4y/3}O_{54}$ microwave dielectric ceramics[J], J. Am. Ceram. Soc. 103 (4) (2020) 2520–2527.
[23] J.D. Breeze, J.M. Perkins, D.W. Mccomb, et al., Do grain boundaries affect microwave dielectric loss in oxides?[J], J. Am. Ceram. Soc. 92 (3) (2010) 671–674.
[24] H. Chen, Z. Xiong, Y. Yuan, et al., Dependence of microwave dielectric properties on site substitution in $Ba_{3.75}Nd_{9.5}Ti_{18}O_{54}$ ceramic[J], J. Mater. Sci. Mater. Electron. 27 (10) (2016) 10951–10957.
[25] J.M. Jehng, I.E. Wachs, Structural chemistry and Raman spectra of niobium oxides [J], ChemInform 3 (15) (2010) 100–107.
[26] H. Zheng, I.M. Reaney, G.D.C. Csete de Gyorgyfalva, Raman spectroscopy of CaTiO3-based perovskite solid solutions[J], J. Mater. Res. 19 (2) (2004) 488–495.
[27] G. Wang, Q. Fu, H. Shi, et al., Suppression of oxygen vacancies generation in $Ba_{6-3x}Sm_{8+2x}Ti_{18}O_{54}$(x=2/3) microwave dielectric ceramics through Pr substitution [J], Ceram. Int. 45 (17) (2019) 22148–22155.
[28] H. Zheng, H. Bagshaw, D. Csete, et al., Raman spectroscopy and microwave properties of $CaTiO_3$-based ceramics[J], J. Appl. Phys. 94 (5) (2003) 2948–2956.
[29] Q. Liao, L. Li, Structural dependence of microwave dielectric properties of ixiolite structured $ZnTiNb_2O_8$ materials: crystal structure refinement and Raman spectra study[J], Dalton Trans. 41 (23) (2012) 6963–6969.
[30] H. Chen, B. Tang, A. Gao, et al., Aluminum substitution for titanium in $Ba_{3.75}Nd_{9.5}Ti_{18}O_{54}$ microwave dielectric ceramics[J], J. Mater. Sci. Mater. Electron. 26 (1) (2015) 405–410.
[31] N. Qin, X.M. Chen, Effects of Sm/Bi co-substitution on microstructures and microwave dielectric characteristics of $Ba_{6-3x}La_{8+2x}Ti_{18}O_{54}$ (x= 2/3) solid solution [J], Mater. Sci. Eng., B 111 (1) (2004) 90–94.
[32] N. Qin, X.M. Chen, Modification of $Ba_{6-3x}Sm_{8+2x}Ti_{18}O_{54}$ (x= 2/3) microwave dielectric ceramics by Nd/Bi Co-substitution on A-site[C]//Key engineering materials 280, Trans Tech Publications Ltd, 2005, pp. 57–60.